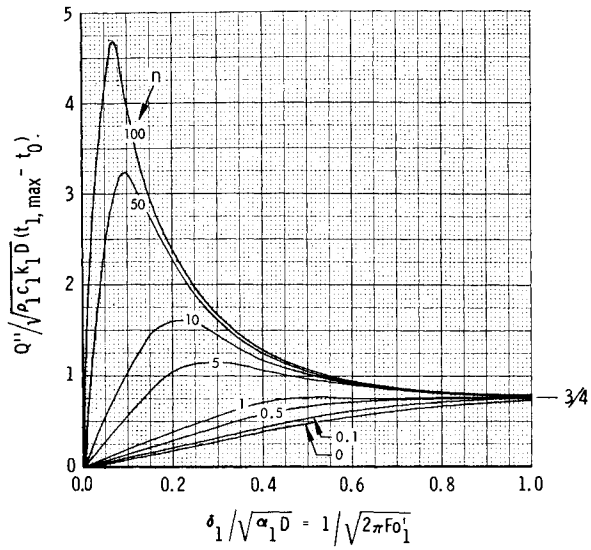

Fig. 8 Maximum heat absorption of single and two-layer plates.

where

$$\frac{T_2(2\pi)}{T_{eq}} = 1 - \frac{1}{12\pi \mathrm{Fo}_1'}\left(\frac{1/n - 3}{1/n - 1}\right) \times \left\{\frac{1 - e^{-6\pi(1/n + 1)\mathrm{Fo}_1'}}{1 - [3(1/n + 1)\mathrm{Fo}_1']^2}\right\}, \quad \mathrm{Fo}_1' \geq 0.0777$$

This integral solution is evidently a poor approximation for the rear-layer response, especially at low values of n.

The time required to reach thermal equilibrium Θ_{eq}, measured from the start of heating, is given in Fig. 7. Equilibration takes longer as the substructure becomes more massive and/or as the outer layer becomes more insulative.

Figure 8 gives a correlation of the heat-sink capability of an insulated substructure in terms of total heat absorbed $Q'' = q''_{max}D/2$ for a maximum permissible exposed-surface temperature rise $t_{1,max} - t_0$. For $n = 0$, increasing thickness increases the total permissible heat load Q'' that can be absorbed without exceeding $t_{1,max}$. This trend continues until the wall becomes thermally semi-infinite, at which point

$$Q'' = (\tfrac{3}{4})(\rho_1 c_1 k_1 D)^{1/2}(t_{1,max} - t_0) \qquad (13)$$

To trace the analogous trend for increasing δ_1 with finite n, it is necessary to imagine δ_2 increasing at the same rate as δ_1 (constant n). At low n and low δ_1 the effect is to first increase Q'' over that where no substructure exists. This increase becomes dramatic for large n, a peak in each curve occurring when δ_1 becomes large enough to overshadow the substructure, and the system becomes self-insulating. Thus, all curves approach the same asymptote ($\frac{3}{4}$) for semi-infinite insulation.

The over-all heat-sink performance of a two-layer plate can exceed that of an equal-weight, single-layer plate of either material. This is accomplished by using an outer layer with a high allowable temperature limit over a second material of lower allowable temperature but higher conductivity. Examples of composites that exhibit this characteristic are oxides over pure metals (e.g., beryllium oxide over beryllium) and pure metal composites such as molybdenum over copper.[1] Considering the latter example with $t_0 = 70°\mathrm{F}$ and $D = 15$ sec, a single copper plate gives $q''_{max} = 1250$ Btu/sec-ft^2, and a single molybdenum plate 1630 Btu/sec-ft^2 if melting is not allowed. The combination of molybdenum over $\frac{1}{2}''$ copper gives $q''_{max} = 1760$ Btu/sec-ft^2, an improvement of 8% at a penalty of 25% increase in section weight (lb/ft^2) over molybdenum alone.

References

[1] Halle, H. and Taylor, D. E., "Transient Heating of Two-Element Slabs Exposed to a Plane Heat Source," CML-59-M-1, May 1959, Chicago Midway Labs., Chicago, Ill.

[2] Mikhaylov, M. D., "Transient Temperature Fields in Shells," TT F-552, June 1969, NASA.

[3] Wilson, L. H., Tucker, M., and Brandt, W. E., "Atmospheric and Hypersonic Phenomena: Entry Problem—Preliminary Heat Sink Design Studies of the Polaris Re-Entry Body," *Proceedings of the 4th U. S. Navy Symposium on Aeroballistics, Bureau of Ordnance, NAVORD 5904*, 1957.

[4] Thomas, P. D., "Approximate Analytical Solutions to Transient Heat Conduction in Finite Slabs With Arbitrary Heat Input," TIAD 148, April 1960, Lockheed Missiles & Space Company, Sunnyvale, Calif.

[5] Schneider, P. J., *Temperature Response Charts*, Wiley, New York, 1963.

[6] Thomas, P. D., "Prediction of Time at Which Surface Melting Begins for a Solid Subjected to Transient Heating," DD 16243, Oct. 1959, Lockheed Missiles & Space Company, Sunnyvale, Calif.

[7] Schneider, P. J. and Wilson, C. F., Jr., "Pulse Heating and Equilibration of an Insulated Substructure," AIAA Paper 70-14, New York, 1970.

Computer Solution to Generalized One-Dimensional Flow

E. William Beans*
Ohio State University, Columbus, Ohio

Introduction

ANY text on gas dynamics describes the simple flow processes which involve only area change, total temperature change, or friction, and a number of methods for solving problems involving all three effects have been presented in the literature; namely, 1) the use of Crocco functions,[1] 2) the use of polytropic exponents,[2] and 3) the use of constant dependent parameters.[3] However, both the Crocco function $pA^{(\epsilon-1)/\epsilon}$ = constant and the polytropic exponent (p/ρ^n = constant) require that ϵ or n be known from experimental data. Here ρ, A, and p are the pressure, area, and density, respectively. Also, the value of ϵ or n is not singularly related to the independent parameters which control the flow, such as total temperature T_0 and area ratio. For example, by varying the pressure ratio across the duct, the Mach number M and pressure distributions will change, even though T_0 and area ratio are unchanged. Hence, the value of ϵ or n will change independent of T_0 and A. The third, use of constant dependent functions, has limitations in that it can only solve problems in which such parameters as temperature or pressure are held constant. Many of these processes are of little practical interest. Also, the use of constant dependent functions specifies the relationship between A, T_0, and friction; hence, generality is lost.

It is possible using electronic computers to apply the method of influence coefficients[4] to one-dimensional flow problems involving simultaneous variations in A, T_0, and friction. The method described here is for the case of fluids having constant composition and a constant ratio of specific heats k. These assumptions are made only for the sake of brevity. The method of influence coefficients as used in fluid mechanics is a set of differential equations obtained from combining the momentum, continuity and energy equations, and equations of state. The only limitations to the method are the assumption

Received June 18, 1970; revision received August 13, 1970.
* Assistant Professor. Member AIAA.

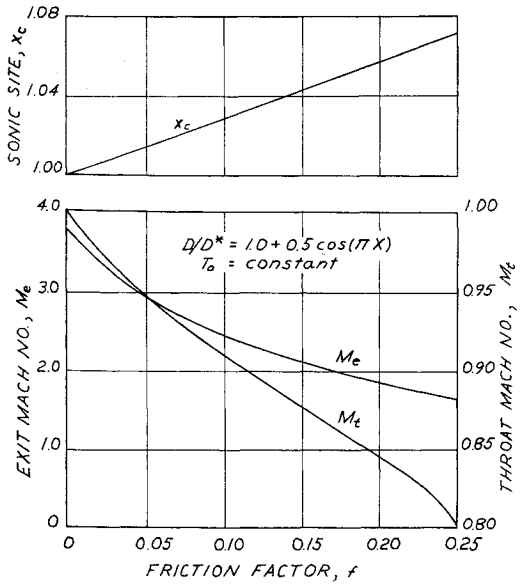

Fig. 1 Variation in flow parameters with friction factor for adiabatic flow, $k = 1.4$.

of one-dimensional flow and the equations of state used to describe the fluid properties.

Numerical examples are presented for flow in a convergent-divergent duct, flows with variation in total temperature, and flow processes which transition from supersonic to subsonic flow in a throatless duct.

Development of Basic Equations

Using the method of influence coefficients[4] one can write for constant composition and k

$$dM^2/M^2 = F_A(dA/A) + F_{T_0}(dT_0/T_0) + F_f(4f dx/D) + F_w(dw/w) \quad (1)$$

The influence coefficients F are functions of M and k only. The independent parameters are A, T_0, friction ($f dx$), and flow rate (w). It is further assumed that the friction factor f is a

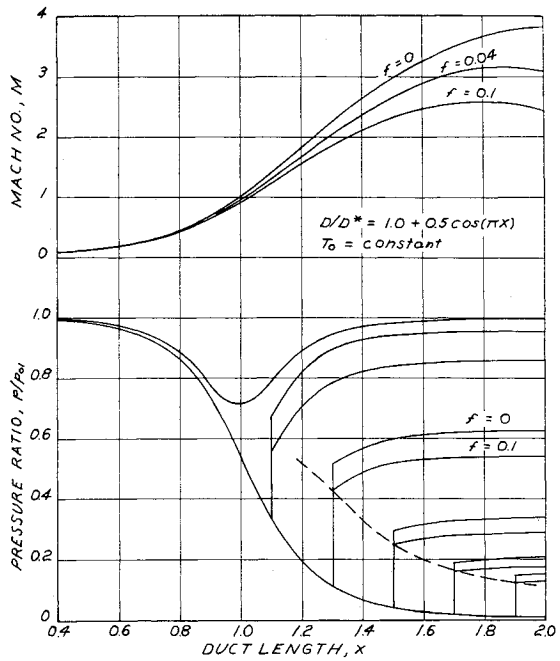

Fig. 2 Adiabatic flow with friction in a convergent-divergent duct, $k = 1.4$.

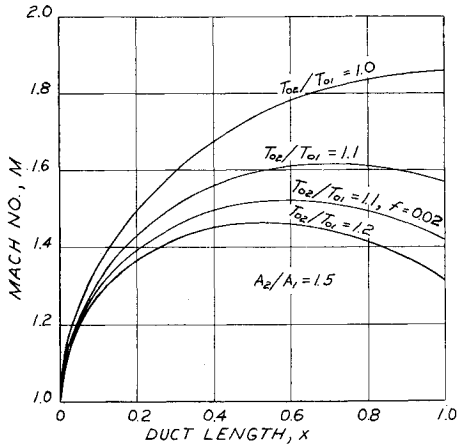

Fig. 3 Supersonic flow in a divergent duct with linear increase in total temperature, $k = 1.4$.

constant, and that the duct has a similar geometric shape at every station, so that the following relation between area and hydraulic diameter D holds

$$(dA)/A = 2(dD)/D \quad (2)$$

In order to solve Eq. (1), one must obtain three additional relations. Let us assume that D, T_0, and w are all functions of the length along the duct x:

$$D = D(x), \quad T_0 = T_0(x), \quad w = w(x) \quad (3)$$

Combining Eqs. (3) and their first derivatives with Eqs. (1) and (2), one obtains

$$dM^2/dx = M^2\psi G(x)/(1 - M^2) \quad (4)$$

where $\psi \equiv 1 + (k - 1)M^2/2$ and

$$G(x) \equiv \left[\frac{-4}{D(x)}\frac{dD}{dx} + \frac{(1 + kM^2)}{T_0(x)}\frac{dT_0}{dx} + kM^2\frac{4f}{D(x)} + \frac{2[1 + kM^2(1 - y)]}{w(x)}\frac{dw}{dx}\right] \quad (5)$$

In Eq. (5) y is the ratio of the velocity of the injected fluid along the axis of the duct to the main stream velocity; y is assumed to be constant for the sake of brevity.

Equation (4) is a nonlinear, first-order differential equation. It was solved numerically using Hamming's Modified Predic-

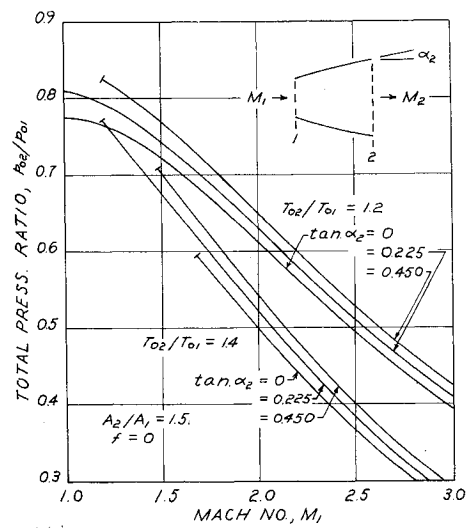

Fig. 4 Effect of duct shape on supersonic flow with linear increase in total temperature, $k = 1.4$.

tor Corrector Method,† which is available as a standard IBM Scientific Subroutine for solving sets of simultaneous nonlinear first-order differential equations and uses a fourth-order Runge-Kutta technique. After $M(x)$ has been determined, the remaining dependent parameters are determined from the following integral relations: $T/T^* = (T_0/T_0{}^*)\phi$, $p/p^* = (w/w^*)(A^*/A)(T/T^*)^{1/2}M$, $u/u^* = M(T/T^*)^{1/2}$, $p_0/p_0{}^* = (p/p^*)\phi^{k/(k-1)}$ and $(s - s^*)/R = [k/(k-1)]\ln(T_0/T_0{}^*) - \ln(p_0/p_0{}^*)$, where $\phi = \psi/\psi^*$. In these relations, $M = 1$ is the reference point, and the parameter at that point is denoted by an asterisk.

Transition of Eq. (4) through the sonic point is accomplished by applying L' Hospital's Rule, which is programed as an integral part of the computer that initially determines the value of x at the sonic point by setting $G(x) = 0$ to make dM^2/dx indeterminate. L' Hospital's Rule is then applied to determine the limiting value for dM^2/dx, so that it will be available when the sonic point is reached. This technique works very well.

Adiabatic Flow with Friction in Convergent-Divergent Duct

A numerical solution to the flow in a convergent-divergent duct with f, T_0 and w constant is illustrated in Figs. 1 and 2, where $D(x)$ is a cosine function. It can be seen from Fig. 1 that the throat Mach number M_t is subsonic, and the sonic point x_c is in the divergent portion of the duct for any value of f. Moreover, M_t and M_e both decrease, and x_c proceeds farther into the divergent portion as f increases. This latter point can easily be illustrated from Eq. (5). At the sonic point

$$G(x) = -(4/D)[(dD/dx) - kf] \tag{6}$$

Since f is always positive, $G(x)$ can only vanish if dD/dx is positive or in the divergent portion. After determining x_c from Eq. (6) the solution to Eq. (4) was then started at $M = 1$ and $x = x_c$ and integrated back to determine the initial conditions by using a negative value for the f. The initial condition and a positive value of f were then used, and the solution to Eq. (4) was obtained by integrating forward through the entire duct.

In Fig. 2, the maximum M is reached before the end of the duct, because dD/dx becomes small near the end of the duct, and $4fkM^2$ becomes the predominant term. Hence, for supersonic flow dM^2/dx becomes negative, and M decreases. Obviously, the divergent portion of a supersonic nozzle should be terminated at the point of maximum M, and this is done in rocket nozzles where an "85% bell" is used. Figure 2 also illustrates flow that includes a normal shock. The changes in properties across the shock are evaluated from the standard one-dimensional shock relations. For a given back-pressure/chamber-pressure ratio, the effect of friction is to move the shock upstream and reduce its strength.

Flow with Variations in Total Temperature

Figure 3 shows $M(x)$ distributions for supersonic flow in a divergent duct with different linear total temperature distributions. The duct shape is parabolic with $A_2/A_1 = 1.5$ and a zero slope at the exit. An example of simultaneous variation in A, T_0, and friction ($f = 0.02$) is presented for comparison. The maximum M does not occur at the exit of the duct, because the change in T_0 is greater than the change in A near the exit for a bell-shaped duct. In other words, the flow behaves as a supersonic Rayleigh line, and M decreases.

A practical design consideration can be drawn from this observation. Some afterburning occurs downstream of the throat in a rocket nozzle. Since $dA/dx \to 0$ near the exit plane, it only takes a little increase in T_0 to cause M to decrease. The thrust of the nozzle, however, increases slightly because there is greater energy release. The variations in thrust and Mach numbers for the processes in Fig. 3 are presented in Table 1. The pressure ratio across the nozzle was taken to be the same for all the processes. The isentropic process ($T_0 = \text{const}, f = 0$) was selected as the standard.

Table 1 Exit conditions for various T_0 distributions; $A_2/A_1 = 1.5$, $M_1 = 1.0$

T_{02}/T_{01}	1.0	1.1	1.2	1.1
f	0	0	0	0.02
M_2	1.855	1.569	1.311	1.417
$M_{\max}$	1.855	1.616	1.461	1.521
F_2/F_{STD}	1.0	1.013	1.112	0.984

The variation of p_{02}/p_{01} with M_1 is presented in Fig. 4 for divergent ducts of different shapes with $A_2/A_1 = 1.5, f = 0$, and linear T_0 distributions (two T_{02}/T_{01}) values are presented). The duct shapes presented are: $\tan\alpha_2 = 0$ — a parabola (bell) with zero exit slope; $\tan\alpha_2 = 0.225$ — a cone with constant slope and; $\tan\alpha_2 = 0.450$ — a parabola (horn) with zero initial slope. The tick marks in Fig. 4 indicate that $M = 1$ was reached somewhere in the duct and the flow is choked. The $M = 1$ point is not always at the entrance or exit. The shape of the duct has a sizeable effect on p_{02}/p_{01}; e.g., at $M_1 = 2.0$ and $T_{02}/T_{01} = 1.2$, the bell has a 6% lower p_{02}/p_{01}, than the horn. It should also be noted, however, that divergence loss from the horn may exceed its gain in total pressure. The results in Fig. 4 are further evidence that ducts with supersonic flow should not be designed with zero exit slopes.

Transition through the Sonic Point

As noted earlier, by specifying that $G(x) = 0$ when $M = 1$, one can generate processes which will vary continuously from $M < 1$ to $M > 1$ and vice versa without going through a throat or through a shock. All these processes require a variation in at least two independent parameters from the group A, T_0, f, and w. There processes also define an implicit relation between the two independent parameters.

Writing Eq. (4) for constant T_0 and constant w one has

$$dM^2/dx = [M^2\psi/(1 - M^2)][(-4/D)(dD/dx) + (4kM^2f/D)] \tag{7}$$

One can obtain a process which will pass continuously through the sonic point by setting the bracketed quantity equal to zero at $M = 1$, or

$$dD/dx = kf \tag{8}$$

which integrates to

$$D/D^* = 1 + kfx \tag{9}$$

where D^* is the duct diameter at $x = 0$. It can be seen from Eq. (9) that the duct is conical. Substituting Eq. (8) into Eq. (7) and simplifying, one obtains

$$dM^2/dx = [M^2\psi/(1 - M^2)]\{[(-1 + M^2)/D](4fdD/dx)\} \tag{10}$$

and

$$dD/D = -dM^2/4M^2\psi \tag{11}$$

It can be seen from Eq. (10) that dM^2/dx will be negative if dD/dx is positive and if $M^2 \neq 1$. Since f is always positive, a supersonic flow will become subsonic in a divergent conic duct. Equation (11) can be integrated to give

$$D/D^* = \varphi^{\frac{1}{2}}/M^2 \tag{12}$$

where D^* has arbitrarily been set at $M = 1$. The relationships for the remaining dependent parameters can be obtained from the aforementioned integral relations. These relation-

† The computer program for solving Eq. (4) and number of the example cases were done by Chin-Wen Wu as part of a thesis[5] under the direction of the author.

Table 2 Flow Relationship for supersonic-to-subsonic processes

Parameter	Variable A & T_0	Variable A & f	Variable A & w	Variable T_0 & f	Variable w & f	Variable[a] A, T_0 & f
A/A^*	$(\varphi/M^2)^{(k+1)/2k}$	$(\varphi/M^2)^{1/2}$	$(\varphi/M^2)^{(k+1/2k)}$	1.0	1.0	$(\varphi/M^2)^{(k+1)/2k\sigma}$
T_0/T_0^*	$(\varphi/M^2)^{1/k}$	1.0	1.0	M^2/ϕ	1.0	$(\varphi/M^2)^{(1-kf/a)/k\sigma}$
$4fx/D^*$	0	$[(4/k)(\varphi/M^2)^{1/4} - 1]$	0	$(k + 1/k) \ln\varphi/M^2$	$[(k + 1)/k] \ln(M^2/\varphi)$	$(4f/a)[(\phi/M^2)^{(k+1)/4k\sigma} - 1]$
w/w^*	1.0	1.0	$(\varphi/M^2)^{1/2k}$	1.0	$(\varphi/M^2)^{1/2}$	1.0
T/T^*	$\frac{1}{M^2}\left(\frac{M^2}{\varphi}\right)^{k-1/k}$	$1/\varphi$	$1/\varphi$	M^2/φ^2	$1/\varphi$	$1/\phi \times (\phi/M^2)^{[(1-kf)/a]k\sigma}$
p/p^*	$1/\varphi$	$1/\varphi$	$1/\varphi$	$1/\varphi$	$1/M^2$	$1/\varphi$
ρ/ρ^*	$(M^2/\varphi)^{1/k}$	1.0	1.0	φ/M^2	φ/M^2	$(M^2/\phi)^{[(1-kf)/a]k\sigma}$
p_0/p_0^*	$\phi^{1/(k-1)}$	$\phi^{1/(k-1)}$	$\phi^{1/(k-1)}$	$\phi^{1/(k-1)}$	$[\phi^{k/(k-1)}]/M^2$	$\phi^{1/(k-1)}$
$(s - s^*)/R$	$[-1/(k - 1)] \times \ln M^2$	$[-1/(k - 1)] \times \ln\phi$	$[-1/(k - 1)] \times \ln\phi$	$[k/(k - 1)] \times \ln M^2 - (k + 1)/(k - 1) \ln\varphi$	$\ln M^2 - [k/(k - 1)] \ln\phi$	$-[(1 - kf/a)]/[(k - 1)\sigma] \times \ln M^2 - [(kf/a)/(k - 1)\sigma] \ln\phi$
dM^2	(−)	(−)	(−)	(−)	(−)	(−)
dA	(+)	(+)	(+)	0	0	(+)
dT^0	(+)	0	0	(−)	0	(+)
fdx	0	(+)	0	(+)	(+)	(+)
dw	0	0	(+)	0	(−)	0
Reversible	yes	no	yes	no	no	no

[a] For a conic duct.

ships plus the relationships for other flow processes which will transit through the sonic point are presented in Table 2. The other flow processes were determined in a similar fashion. Table 2 also presents the direction of change for M for a positive change in each independent parameter, and whether the process can be reversed. The variation in $(s - s^*)/R$ with M for these processes is presented in Fig. 5, which shows that the processes are thermodynamically possible because at $M = 1$, $ds/dM \neq 0$ and is positive for all irreversible processes. The variable w and f process cannot proceed from either the $M < 1$ or $M > 1$ side beyond $M = 1.414$ because $ds/dM = 0$ at that point. This result is similar to those predicted by the Crocco functions.

Flow processes which pass through $M = 1$ can be developed for variations in three independent parameters if an arbitrary relationship between two parameters is assumed. For example, we assume a conic duct shape $(D/D^* = 1 + ax)$, substitute this function for $D = D(x)$ into Eq. (5), set Eq. (5) equal to zero at $M = 1$, integrate and obtain

$$T_0/T_0^* = (1 + ax)[4(1 - kf/a)/(k + 1)] \quad (13)$$

Equation (13) is substituted into Eqs. (4) and (5) to give

$$dM^2/M^2\psi = (-4/(k + 1)[(a + f)dx/(1 + ax)] \quad (14)$$

which can be integrated in a closed form to produce

$$D/D^* = (\varphi/M^2)[(k + 1)/4\sigma]^{(k+1)/4\sigma} \quad (15)$$

where $\sigma = 1 + f/a$. Equation (15) and the relationship for the dependent parameters are presented in Table 2. Equations (13–15) indicate that one can design an experiment which will demonstrate transition through the sonic point in a throatless duct.

The variations in A and T_0 with M in a conic duct for various values of f/a are presented in Fig. 6. In turbulent flow, f is typically in the range of 0.001 to 0.01. It can be seen from

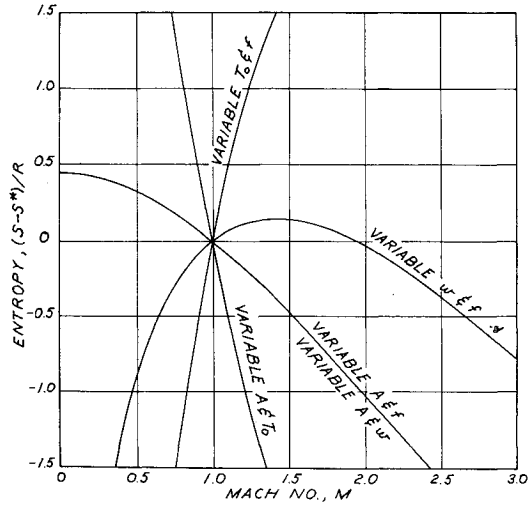

Fig. 5 Flow processes for continuous transition from supersonic-to-subsonic flow, $k = 1.4$.

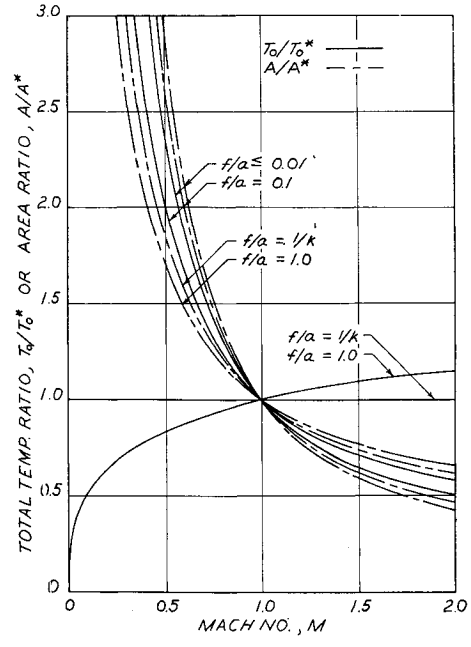

Fig. 6 Variation in area, total temperature and friction for transitional flow in a conic duct, $k = 1.4$.

Table 3 Points of $ds/dM = 0$ for subsonic to supersonic flow, $k = 1.4$

f/a	$1/k$	0.8	0.9	1.0	2.0	4.0	10.0	∞
M	0	0.577	0.828	1.0	1.73	2.15	2.42	2.65
$(s - s^*/R)_{max}$	0.455	0.131	0.026	0	0.498	1.25	1.94	∞

Fig. 6 that the value of f has little effect on the flow in moderately divergent duct. For duct half-angles greater than 6°, f/a will be less than 0.1. This is a further indication that since the absolute value of f is an unknown factor, an experiment can be designed which will pass from supersonic to subsonic flow.

At larger values of f/a or in ducts with very little divergence, the effect of friction becomes much more prominent. In fact, at $f/a = 1/k$, T_0 is constant, see Eq. (13). This case is, of course, the variable A and f process described in Fig. 5. It is also worth noting that $f/a = 0$ corresponds to the variable A and T_0 process, and that $f/a = \infty$ corresponds to the variable T_0 and f process in Fig. 5. The variations in A and T_0 with between $f/a = 0$ and $f/a = 0.10$ are too small to be seen in Fig. 6. The variations in A and T_0 are 1% or less and 2% or less, respectively, between Mach 0.5 to 3.0.

At $f/a \geq 1/k$, $ds/dM = 0$ at some point in the flow. This behavior is also similar to that predicted by the Crocco functions. Heating or increase in T_0 is required at $M < Ms_{max}$, and vice versa. This point is illustrated in Fig. 6 for $f/a = 1.0$. For $f/a > 1$, the point of $ds/dM = 0$ occurs at $M > 1$. The values of M and entropy at the $ds/dM = 0$ point is presented in Table 3 for various values of f/a.

References

[1] Dobrowolski, A., "Analysis of Nonconstant Area Combustion and Mixing in Ramjet and Rocket-Ramjet Hybrid Engines," TND-3626, 1966, NASA.

[2] Brandt, A., "One-Dimensional Combustion Optimization," AIAA Paper 68-644, Cleveland, Ohio, June 1968.

[3] Beans, E. W., "Compressible Flow Processes Involving Area, Friction and Total Temperature Change," *Journal of Spacecraft and Rockets*, Vol. 6, No. 3, March 1969, pp. 331–333.

[4] Shapiro, A. H., *The Dynamics and Thermodynamics of Compressible Fluid Flow*, Vol. 1, Ronald Press, New York, 1953, pp. 219–260.

[5] Wu, C.-W., "A Numerical Approach with Digital Computation to Generalized One-Dimensional Flow," M.S. thesis, Dept. of Mechanical Engineering, The Ohio State Univ., Columbus, Ohio.

Outgassing Behavior of Multilayer Insulation Materials

A. P. M. GLASSFORD*

Lockheed Missiles & Space Company, Palo Alto, Calif.

MULTILAYER insulation systems show minimum effective thermal conductivity when they are operated with an interlayer gas pressure below 10^{-5} torr, at which pressure the gaseous heat conduction is negligible. In service this low pressure is reached by evacuation of the interlayer gas to space or by vacuum pump. As the gas pressure is reduced, however, outgassing from the insulation surfaces can seriously prolong the evacuation period. This Note reports some experimental outgassing data[1] for multilayer insulation materials under conditions appropriate to use in cryogenic fuel tanks. For such a system, the multilayer insulation would be purged before launch with a gas not condensible at the fuel temperature, such as helium. With the purge gas pressure held at 1 atm the fuel tank would be filled, and the insulation wrap would assume a temperature between ambient and the fuel temperature. During and after launch the purge helium gas would be evacuated to space.

The data are reported as recommended by the American Vacuum Society's AVS-9,[2] according to which the solid involved is to be described only by its gross characteristics of manufacturing history, pretreatment, etc., and the data are to be obtained and presented as mass released per unit time per unit solid apparent surface area or bulk volume as a function of time for constant experimental temperature and negligible experimental pressure. Guidelines are proposed by AVS-9 for apparatus sizing and design to ensure that the background outgassing due to the apparatus itself is negligible, and that the experimental gas pressure is negligible with respect to the ambient pressure. Because of the peculiarities of the sample geometry and the required preconditioning, these two guidelines could not be followed strictly in this work, but preliminary experiments were conducted to confirm that the intent of the guidelines had been met.

The pumpdown technique selected consists of evacuating in turn and under the same conditions an empty chamber and then the chamber plus insulation sample. The sample outgassing rate is found from the difference in the slopes of the two pressure histories at a given chamber pressure. The mass balance equations for the empty chamber and the chamber plus samples are, respectively,

$$-(V/RT)(dP/dT)_c = SP/RT - Q_cA_c \quad (1)$$

$$-(V/RT)(dP/dT)_s = (SP/RT) - Q_cA_c - Q_sA_s \quad (2)$$

If the chamber outgassing rate Q_c is negligible, the volumetric pumping speed S is constant or a function only of P over the experimental pressure range, and the temperature T is constant during the experiment, then the sample outgassing rate Q_s may be found by subtracting Eq. (2) from Eq. (1) at constant pressure. This gives

$$Q_s = -V/A_sRT\,[(dP/dt)_c - (dP/dt)_s]_{P=\text{constant}} \quad (3)$$

This value of Q_s is assigned to the time at which $(dP/dt)_s$ was measured.

Outgassing quantities are presented here in the customary units of pressure times volume. These data can be converted to mass quantities by dividing by the gas constant times the measurement temperature, which was 297°K for the reported tests.

Apparatus

The insulation sample chamber (Fig. 1) is 6 in. in diameter and 1.5 in. high, and its top is closed by the underside of a tank 6 in. diam and 3 in. deep. The joint is sealed by a vacuum flange using either a copper gasket at the lower temperatures or an O-ring gasket at temperatures closer to ambient. The chamber and most other components communicating with it are made from polished stainless steel. The tank can be filled with a boiling or melting mixture to provide a constant temperature heat sink or source. A sample tray within the sample chamber supports the insulation sample. The insulation sample sheets, cut 5.4 in. o.d. and 0.5 in. i.d., are stacked on the tray to a height such that when the chamber is closed, the underside of the tank exerts very little pressure on the stack, establishing its height at 0.40 in. Thermocouples were positioned within the sample stack at three

Received July 6, 1970; revision received August 13, 1970. This work was sponsored by NASA/Marshall Space Flight Center as a part of Contract NAS 8-20758.

* Research Scientist, Engineering Sciences Laboratory.